Active nematic fluids with flow alignment

Author: Pablo Romero Marimon*
Facultat de Física, Universitat de Barcelona, Diagonal 645, 08028 Barcelona, Spain.

Advisor: Jaume Casademunt Viader
(Dated: February 5, 2021)

Abstract: We derive a stream function formulation for the dynamics of 2D active nematics in the absence of topological defects. This formulation extends previous studies by incorporating the flow alignment coupling. We study the linear stability analysis of the spontaneous-flow instability and check it numerically. Then, we obtain numerically the 2D nonlinear stationary states for a particular limit in which active forces dominate over elastic ones, and viscous dissipation dominates over rotational dissipation. Finally, we find significant differences with previous results due to the presence of the flow alignment coupling.

I. INTRODUCTION

In recent years, several advances have been made within the context of fluid dynamics in active matter. An active system is a nonequilibrium condensed system composed of large numbers of active "agents", each capable of converting both stored and ambient free energy into movement or mechanical forces. These complex systems are of high interest in biophysics, since many remarkable examples are biological in origin, such as bacteria and self-organising bio-polymers. A thorough description of soft active matter can be found in M. C. Marchetti et al. [1] and in the references therein.

Specifically, we focus on "active gels", a type of active matter which consists of orientable and elongated active particles suspended in a fluid medium. Furthermore, we consider the nematic case, where the active particles themselves are head-tail symmetric. Therefore, the final equations of this model will be invariant under **p** to **-p** transformations, being **p** the polarisation vector.

The work presented in here is subsequent to the paper of R. Alert et al. [2], which aims to study the phenomenon of turbulence in active gels. In fact, they provide a universal scaling law for active matter, where the kinetic energy is shown to be $E(q) \sim q^{-1}$ at long wavelengths. Although Kolmogorov's scaling law $E(q) \sim q^{-5/3}$ for non active matter dates back to 1941 (see [3]), the existence of universal scaling properties in active flows has remained unclear until now, and several fundamental questions remain unsolved.

The minimal model introduced in [2], designed to capture universal properties of turbulence, was not fully realistic. In particular, it did not include the flow alignment coupling measured by the parameter $\boldsymbol{\nu}$, which measures the tendency of the orientation **p** to align with the flow and at the same time the shear stress generated by a distorted orientation of the field **p** (see R. Voituriez et al. [4]).

Hence, to assess the claim of universality of nematic turbulence, a model of active gel including this transport coefficient needs to be developed. To this end, we include this coefficient into the constitutive equations and conservation laws, which allows us to obtain the equations ruling the system of an active nematic gel with the flow alignment effect. Afterwards, an adaptation of the numerical algorithm implemented by R. Alert in [2] is performed in order to integrate the dynamics of the system. Nevertheless, the new model with the added parameter turns to increase significantly the complexity of implementing a numerical integration, so, in this work, we focus on a particular limit of parameters.

II. MINIMAL MODEL OF ACTIVE NEMATICS

Let us consider a 2D active incompressible nematic in a domain of area L^2, viscosity η, frictional drag γ and alignment coefficient ν. Let the polar field be given by the unit director vector $p_\alpha = (\cos\theta, \sin\theta)$. We assume that p_α has constant modulus and that the field θ is not singular, that is, we exclude topological defects. As shown in K. Kruse et al. [5], the continuity equation for the conservation of linear momentum reads

$$\rho(\partial_t + v_\beta\partial_\beta)v_\alpha = -\partial_\alpha P + \partial_\beta(\sigma_{\alpha\beta} + \sigma^a_{\alpha\beta}) \qquad (1)$$

where ρ is the density, v the velocity, P the pressure and the symmetric and antisymmetric parts of the stress tensor are

$$\sigma_{\alpha\beta} = 2\eta v_{\alpha\beta} - \zeta q_{\alpha\beta} + \frac{\nu}{2}(p_\alpha h_\beta + p_\beta h_\alpha - p_\gamma h_\gamma \delta_{\alpha\beta}),$$
$$\sigma^a_{\alpha\beta} = -\frac{1}{2}(p_\alpha h_\beta - p_\beta h_\alpha),$$

respectively, being ζ the active flow coefficient, h_α the molecular field, $v_{\alpha\beta} = \frac{1}{2}(\partial_\alpha v_\beta + \partial_\beta v_\alpha)$ and $q_{\alpha\beta} = p_\alpha p_\beta - \frac{1}{2}p_\gamma p_\gamma \delta_{\alpha\beta}$. For vanishing Reynolds numbers we have that the left side in (1) also vanishes. Then, taking the curl in (1) for RE=0 we obtain

$$\mathrm{curl}(\sigma_{\alpha\beta} + \sigma^a_{\alpha\beta}) = 0, \qquad (2)$$

*Electronic address: romerompablo@gmail.com

since curl$(\partial_\alpha P)$ also vanishes as it is the curl of a gradient.

Now, we proceed to take the curl separately to the symmetric and antisymmetric parts of the stress tensor. With this aim, we firstly recall that the molecular field is defined as $h_\alpha = K\nabla^2 p_\alpha + h_\parallel^0 p_\alpha$ where K is a constant and $h_\parallel^0$ a Lagrange multiplier (see K. Kruse [5]). For simplicity, we consider a local rotation in order to work with the axis given by the parallel and perpendicular components of the molecular field to the vector p_α. Indeed, the relation between both frames of reference is given by a well-known rotation matrix in the plane.

Then, we need to find the expressions of $h_\parallel$ and $h_\perp$. Since the definition of the molecular field contains a Lagrange multiplier involving only the parallel component, $h_\perp$ can be easily obtained from the projection of $K\nabla^2 p_\alpha$ in the perpendicular axis, which leads us to $h_\perp = K\nabla^2\theta$.

On the other hand, due to the presence of the Lagrange multiplier, we cannot proceed as before to obtain the parallel component. Alternatively, $h_\parallel$ can be obtained from the constitutive equation (see R. Voituriez [4])

$$\frac{dp_\alpha}{dt} = \frac{1}{\gamma}h_\alpha - \nu p_\alpha v_{\alpha\beta} \tag{3}$$

where $\frac{dp_\alpha}{dt} = \vec{v}\cdot\vec{\nabla}p + \partial_t p + \omega_{\alpha\beta}p_\beta$ and $\omega_{\alpha\beta} = \frac{1}{2}(\partial_\alpha v_\beta - \partial_\beta v_\alpha)$. After some straightforward yet tedious calculations, $h_\parallel$ can be isolated from (3) to obtain that

$$h_\parallel = \frac{\gamma\nu}{2}\left(\sin 2\theta(\partial_y^2\psi - \partial_x^2\psi) + 2\cos 2\theta\partial_{xy}^2\psi\right). \tag{4}$$

Thus, introducing the stream function ψ such that $v_x = \partial_y\psi$ and $v_y = -\partial_x\psi$ Eq. (2) finally reads

$$\begin{aligned}\eta\nabla^4\psi + \frac{1}{2}K\nabla^4\theta + \nu B(\theta) = \\ \zeta\left(\frac{1}{2}(\partial_y^2 - \partial_x^2)\sin 2\theta + \partial_{xy}^2\cos 2\theta\right)\end{aligned} \tag{5}$$

with $B(\theta) = \frac{1}{2}(\partial_y^2 - \partial_x^2)(h_\parallel \sin 2\theta + K\nabla^2\theta\cos 2\theta) + \partial_{xy}^2(h_\parallel\cos 2\theta - K\nabla^2\theta\sin 2\theta)$.

To obtain a closed system of equations, we need to consider another equation for p_α. Taking it from K. Kruse [5], we have that

$$(\partial_t + v_\beta\partial_\beta)p_\alpha + \omega_{\alpha\beta}p_\beta = \frac{1}{\gamma}h_\alpha - \nu v_{\alpha\beta}p_\beta \tag{6}$$

where we neglected the active alignment term proportional to p_α. Multiplying the vectorial Eq. (6) by $p_\alpha^\perp = (-\sin\theta, \cos\theta)$ and rewriting each term we finally get

$$\partial_t\theta - \frac{K}{\gamma}\nabla^2\theta + \frac{1}{2}\nabla^2\psi = (\partial_x\psi)(\partial_y\theta) - (\partial_y\psi)(\partial_x\theta) - \nu C(\theta) \tag{7}$$

where $C(\theta) = \frac{1}{2}\cos 2\theta(\partial_y^2\psi - \partial_x^2\psi) - \sin 2\theta\partial_{xy}^2\psi$.

Eqs. (5,7) define our dynamical system. It is easy to see that setting $\nu = 0$ leads us to the model used in R. Alert [2].

A. Linear regime and dimensionless form

It is clear that Eqs. (5,7) have a trivial homogeneous solution with $\theta = 0$, $\psi = 0$. Here we perform the linear stability analysis of this state which leads to spontaneous flow. To this end, let us consider a perturbation of wavevector $\vec{q}$ forming an angle ϕ with p_x. Then, substituting the linear ansatzes $\theta = \theta_0\exp\{i(q_x x + q_y y) + \Omega t\}$ and $\psi = \psi_0\exp\{i(q_x x + q_y y) + \Omega t\}$ in Eqs. (5,7) and linearizing them in terms of θ_0 and ψ_0, the linear growth rate $\Omega(q)$ of the perturbation can be isolated. Whenever the linear growth rate is positive, the perturbation is unstable since its amplitude increases.

In fact, considering that $q_x = q\cos\phi$ and $q_y = q\sin\phi$, the linearized equations respectively read

$$\begin{aligned}\theta_0\left(\frac{1}{2}Kq^4 + \frac{1}{2}K\nu(q_y^4 - q_x^4) + \zeta(q_y^2 - q_x^2)\right) \\ + \psi_0\left(\eta q^4 + \gamma\nu^2 q_x^2 q_y^2\right) = 0,\end{aligned} \tag{8}$$

$$\theta_0\left(\Omega + \frac{K}{\gamma}(q_x^2 + q_y^2)\right) = \psi_0\left(\frac{1}{2}(q_x^2 + q_y^2) - \frac{1}{2}\nu(q_x^2 - q_y^2)\right). \tag{9}$$

Now, properly combining Eqs. (8,9) the growth rate can be written as follows

$$\begin{aligned}\Omega = -\frac{K}{\gamma}q^2\left(1 + \frac{\gamma(1-\nu\cos 2\phi)^2}{4\eta\left(1 + \frac{\gamma}{4\eta}\nu^2\sin^2 2\phi\right)}\right) \\ + \frac{\zeta}{2\eta}\frac{\cos 2\phi(1-\nu\cos 2\phi)}{1 + \frac{\gamma}{4\eta}\nu^2\sin^2 2\phi}.\end{aligned} \tag{10}$$

It is convenient for the subsequent work to consider a scaling of the equations in order to reduce the amount of parameters of the system. With this aim, let us scale the lengths by L, the time by $\gamma L^2/K$ and the stresses by K/L^2. Furthermore, let us denote $r = \gamma/\eta$ and define the activity parameter as

$$A = \frac{\mathcal{S}|\zeta|L^2}{K}r \tag{11}$$

where $\mathcal{S} = -1(+1)$ for contractile (extensile) stresses. The marginal curves $\Omega = 0$ plotted in Fig. (1) represent the boundary between linearly stable and unstable modes in dimensionless variables. Indeed, it shows a substantial change when $\nu > 1$, what is called the flow alignment regime, since this effect begins to be relevant. Specifically, some of the parallel modes are in that case unstable, as opposed to the flow tumbling regime for $\nu < 1$.

B. Viscous dissipation limit with A finite

Due to the complexity of solving numerically the system given by Eqs. (5,7), we focus on the particular case

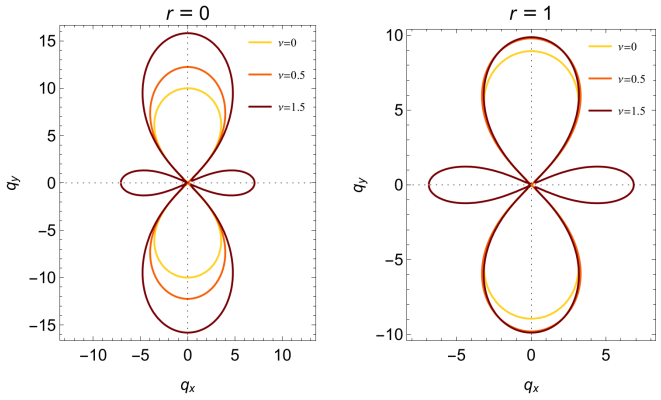

FIG. 1: Marginal curves $\Omega = 0$ considering the scaling mentioned above, for $r = 0$ (left) and $r = 1$ (right). The inner regions represent the unstable modes in the Fourier space, since $\Omega > 0$. In all cases, the activity is set to $A = -200$.

where $\gamma \gg \eta$ ($r \to 0$) while keeping the activity finite. This stands to the physical limit where the viscous dissipation dominates over the original from the nematic and active stresses dominate over elastic stresses. After applying the scaling mentioned in Sec. II A, in this limit Eqs. (5,7) read

$$\nabla^4 \psi = A \left(\frac{1}{2} (\partial_y^2 - \partial_x^2) \sin 2\theta + \partial_{xy}^2 \cos 2\theta \right), \tag{12}$$

$$\partial_t \theta = \nabla^2 \theta - \frac{1}{2} \nabla^2 \psi + (\partial_x \psi)(\partial_y \theta) - (\partial_y \psi)(\partial_x \theta) - \nu C(\theta). \tag{13}$$

Given that these equations depend on the flow alignment coefficient, this plays a role in the dynamics even when $\gamma \gg \eta$ (and A is finite). Hence, an analysis of these equations will provide new insight into the dynamics in active gels not shown in [2]. Furthermore, Fig. (1) illustrates that in the linear regime, the system behaves similarly for $r = 0$ and r finite, which also justifies that this limit is meaninguful.

III. NUMERICAL APPROACH

To fully understand the behaviour of the system given by (12,13) a numerical integration of these equations is required. To this end, we used the algorithm implemented by R. Alert in [2] as starting point and adapted the routines therein to solve the system of our interest.

The resulting algorithm is a combination of spectral methods and finite differences that discretely integrates the equations in a n^2-nodes square lattice of side $L = 1$ given a sinusoidal initial condition $\theta(\vec{r}, 0) = \theta_0 \sin(\vec{r} \cdot \vec{q})$. The procedure consists of a certain amount k of steps, integrating in each one a discrete time dt. In each step, given the polar field, the stream function is firstly computed in the Fourier space. In fact, it yields from the Eq. (12) and from the properties of the Fourier transform that the Fourier transform of the stream function is given by

$$\mathcal{F}[\psi]_{\vec{q}}(t) = \frac{A}{q^4 + \epsilon} \left(\frac{q_x^2 - q_y^2}{2} \mathcal{F}[\sin 2\theta]_{\vec{q}} - q_x q_y \mathcal{F}[\cos 2\theta]_{\vec{q}} \right) \tag{14}$$

where the term $\epsilon = 10^{-8}$ is set to avoid the divergence in the origin. Therefore, the stream function can be obtained by computing the inverse Fourier transform of the Eq. (14).

Once having the value of ψ for every point of the lattice, the algorithm finds $\dot{\theta}$ using finite differences the same way as in [2]. However, since now the term $C(\theta)$ in Eq. (13) contains the crossed derivative $\partial_{xy}^2 \psi$, a prescription is needed to compute this quantity. Within the framework of finite differences, we have that

$$\partial_{xy}^2 \psi(i,j) = \frac{\psi(i+1,j+1) - \psi(i+1,j-1)}{4\Delta Y \Delta Y} - \frac{\psi(i-1,j+1) + \psi(i-1,j-1)}{4\Delta Y \Delta Y} \tag{15}$$

being $\psi(i,j)$ the stream function in the point (i,j) and ΔX, ΔY the distances between consecutive points in each axis. Lastly, the new polar field is defined as $\theta_{t+dt} = \theta_t + \dot{\theta} dt$ for every point in the lattice.

In the simulation we also include some noise added in every step, to incorporate physical fluctuations, from either thermal or active origin. Besides, this also helps the numerical system to escape from unstable or metastable states.

A. Testing the linear regime

The growth rate can be used as a test to check the proper behaviour of the linear terms in the algorithm. To this end, recalling the scaling and the physical limit introduced in Sec. II A the growth rate can be written as

$$\Omega = -q^2 + \frac{A}{2} \cos 2\phi \, (1 - \nu \cos 2\phi). \tag{16}$$

Then, the growth rate can be obtained analytically using the expression (16) and computationally by computing $\dot{\theta}/\theta$ in every point of the lattice. In fact, Fig. (2) shows high accuracy between the theoretical values of the growth rate and the numerical computation, for some of the transversal modes. This validates the numerical scheme at least at linear level.

B. Simulation parameters

In all the simulations we have focused on contractile stresses ($\mathcal{S} = -1$) and considered activity parameters $|A|$ from 200 to 800. The mode of the initial condition was taken as $q_x = 0$, $q_y = 2\pi$ and its amplitude was

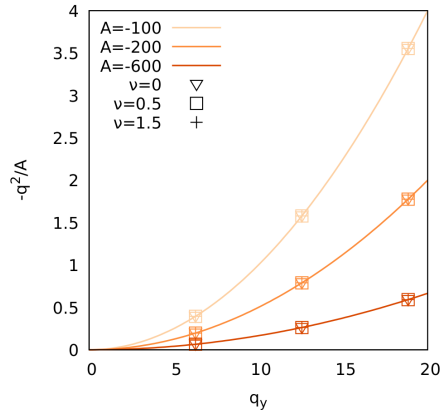

FIG. 2: Validation of the growth rate for the transversal modes. The curves represent $-q^2/A$, while the points represent the quantity $\frac{\Omega}{A} - \frac{1}{2}\cos 2\phi(1 - \nu \cos 2\phi)$ for the corresponding A, ν, q_y and value of Ω obtained computationally.

$\theta_0 = 0.07854$. The time step used was $dt = 3 \cdot 10^{-6}$. This was conditioned by the fact that a smaller value would increase the simulation time, while a much bigger one may lead to numerical instabilities.

All the simulations shown in the next section are in a lattice with $n = 256$. However, since a direct integration with that resolution was not feasible due to the high computational time required, we proceeded as follows: firstly, for every A and ν the stationary state was found in a lattice of 128×128. Afterwards, the resulting polar field was used to obtain a linear interpolation of this field in a lattice of $n = 256$, which was used as initial condition to run a simulation in this resolution. Of course, since this state was already close to the stationary state, this was reached in a relatively short time.

IV. NUMERICAL RESULTS

For all the combinations of the parameters A and ν considered, we reached stationary states (see Fig. (3)). Hence, our regime is far from being chaotic. Instead, the phenomenon of active turbulence should appear for higher values of the activity parameter, as seen in R. Alert [2].

However, there are noticeable differences between the stationary states for different flow alignment coefficients when the activity increases. For $\nu = 0$ and low activity ($|A| = 200$) the stationary state shows one full oscillation in the y direction, which corresponds to the most linearly unstable mode (the dominant one). Still for $\nu = 0$, Fig. (3) shows how more complex zig-zag patterns are formed for $|A| = 400$ and become fuzzier when increasing the activity even further. Nonetheless, it seems clear that the zig-zag states correspond to secondary instabilities of the horizontal bands.

On the other hand, for $\nu > 0$ these bands are not stationary. Instead, for $|A| = 400$ oblique bands appear defining an angle of $\phi = \pi/4$ with the x axis. This pattern corresponds to the mode $q_x = q_y = 2\pi$, which is linearly stable since for this mode $\Omega < 0$. Thus, the stationary states having oblique bands yield from the nonlinear part of the equations, which are responsible for exciting this mode.

Lastly, it is also noticeable that when the activity increases for $\nu > 0$ and the bands are no longer stationary, the resulting patterns are a perturbation of the oblique bands.

Afterwards, we carried a simulation for $|A| = 600$ and $\nu = 0$, taking the stationary state for $|A| = 600$ and $\nu = 1.5$ as initial condition. The resulting stationary state was slightly modified in terms of the amplitude but conserved the oblique bands. We conclude that these bands are also solutions of the $\nu = 0$. These were never found before, implying that they coexist with other stationary patterns, with different basin of attraction. In fact, being this a nonequilibrium system, it is hard to address analytically which state is more stable.

Another interesting conclusion we can draw from these simulations involves also the stream function. If we now take Eqs. (12, 13) for $\nu = 0$ and consider a solution of

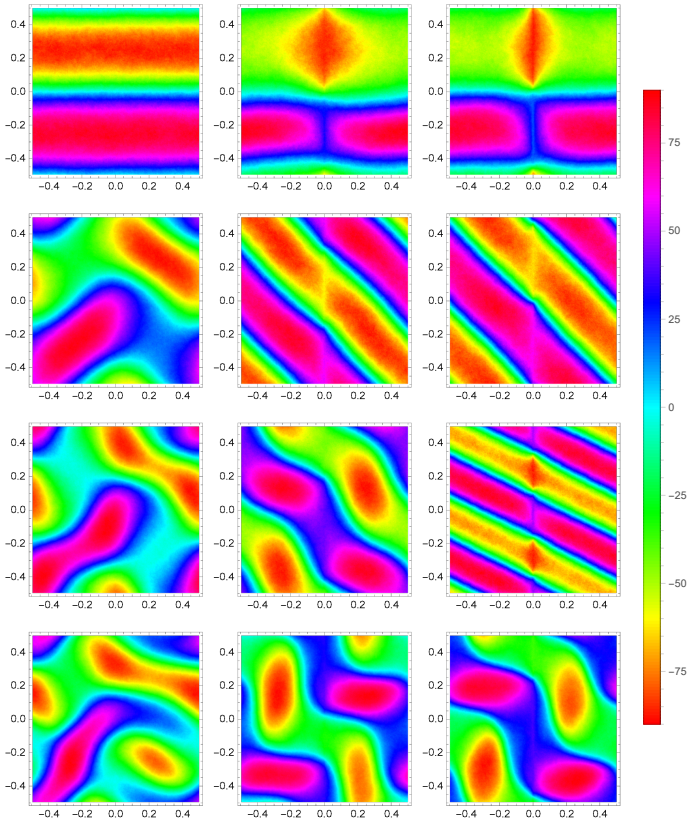

FIG. 3: Polar field of the stationary states in a 256×256 lattice represented in degrees. The rows correspond to the four values of $|A|$, from 200 to 800 in increments of 200 from top to bottom and the columns show values of $\nu = 0$, 0.5 and 1.5 from left to right.

the form $\psi = \mathcal{K}\theta$ being $\mathcal{K}$ a constant, it can be seen that such a solution can be a stationary state for a suitable value of $\mathcal{K}$. In fact, imposing that $\partial_t\theta = 0$ in the second and computing the derivatives, we obtain that

$$\nabla^2\theta\left(1 - \frac{\mathcal{K}}{2}\right) = 0. \tag{17}$$

Hence, for $\mathcal{K} = 2$ this does not imply a condition on the polar field. Therefore, we can select θ to fulfil the Eq. (12) with $\psi = \mathcal{K}\theta$. It follows from here that θ and $\psi = 2\theta$ can be a stationary solution.

It is clear that whenever the polar field and the stream function are proportionals, their contour lines will be equal. Therefore, from Fig. (4) we know that the stationary solution found for $|A| = 800$ and $\nu = 0$ is of the form described above, since the lines where the polar field is constant coincide with streamlines.

On the other hand, for $\nu > 0$ the term $-\nu C(\theta)$ prevents the solutions θ and $\psi = 2\theta$ from being stationary in general. Thus, in this case the contour lines do not have to coincide (see Fig. (4)).

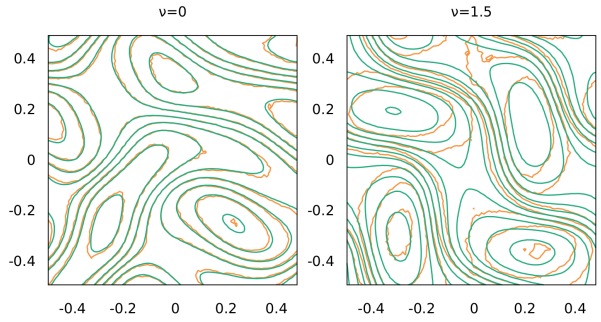

FIG. 4: Contour lines of the stationary state for $|A| = 800$ and $\nu = 0$ (left) and $\nu = 1.5$ (right). The orange lines represent curves where the polar field is constant, whereas the green lines are curves of constant stream function.

V. DISCUSSION AND CONCLUSIONS

In summary, we have introduced a new theoretical model of a 2D active nematic that considers the flow alignment effect and have derived the equations ruling the dynamics of such a system. These new equations show consistency with previous papers, leading to the same expressions when $\nu = 0$. Nonetheless, the new parameter clearly increases their complexity introducing new nonlinearities.

By linearizing these equations, we obtained the expression of the growth rate coefficient, which allows us to study the stability at linear order. We also showed a notable change for $\nu > 1$ (the flow alignment regime), since some of the parallel modes happen to be unstable, contrary to the case of $\nu = 0$.

Then, due to the complexity of the resulting equations, we focused on the limit where $r \to 0$ keeping A finite. By introducing some adjustments in the software made by R. Alert in [2] we have been able to integrate numerically the dynamics for low activity parameters. As expected, the regime was not chaotic and the stationary states were obtained and discussed for $\nu = 0$ and $\nu > 0$. Besides, we showed remarkable differences when considering a finite flow alignment coefficient. We found new stationary states formed by oblique bands for all cases of ν, and more complex 2D patterns for $\nu > 0$ that differ from their counterparts for $\nu = 0$. In addition, we found that the contour lines of the polar field and the stream function were not equal, as used to happen for $\nu = 0$.

Although the active turbulence is much beyond the scope of this work, this serves as a starting point to understand this phenomenon considering the flow alignment effect, which has been shown that significantly affects the dynamics of the system. Of course, the general case with non vanishing r has yet to be addressed. To this end it is advisable to consider a finite elements method for the numerical integration, since the explicit method used in here can hardly be adapted to face the general case. This, together with an exploration for higher values of the activity parameter, will provide new insight into the phenomenon of active turbulence.

Acknowledgments

First and foremost, I would like to express my gratefulness to my advisor, Dr. Jaume Casademunt for the continuous support and guidance that he provided me throughout all the project. Also, to Dr. Ricard Alert for the codes and having answered my questions. Finally, to my family, my friends and especially to Marta. Thanks for your unconditional support during these years.

[1] M. C. Marchetti, J. F. Joanny, S. Ramaswamy, T. B. Liverpool, J. Prost, and R. Aditi Simha. *Hydrodynamics of soft active matter*. Mod. Phys, **85**, 1143–, (2013).

[2] R. Alert, J. F. Joanny and J. Casademunt. *Universal scaling of active nematic turbulence*. Nature Physics, **16**, 682–688, (2020).

[3] A. N. Kolmogorov, in *Proceedings of the Royal Society A,* **434**, 9-13, (1991).

[4] R. Voituriez, J. F. Joanny and J. Prost. *Spontaneous flow transition in active polar gels*. Europhys. Lett., **70**, 404-410, (2005).

[5] K. Kruse, J.F. Joanny, F. Jülicher, J. Prost, and K. Sekimoto. *Generic theory of active polar gels: a paradigm for cytoskeletal dynamics*. Eur. Phys., **16**, 5-16, (2005).